Temperature dependent refractive index and absorption coefficient of congruent lithium niobate crystals in the terahertz range

Xiaojun Wu,[1,3,*] Chun Zhou,[1,2] Wenqian Ronny Huang,[4] Frederike Ahr,[1,2] and Franz X. Kärtner[1,2,3,4]

[1] *Center for Free-Electron Laser Science, Deutsches Elektronen Synchrotron (DESY), Hamburg 22607, Germany*
[2]*Department of Physics, University of Hamburg, Hamburg 20148, Germany*
[3]*The Hamburg Center for Ultrafast Imaging, Hamburg 22607, Germany*
[4]*Department of Electrical Engineering and Computer Science, Research Laboratory of Electronics, Massachusetts Institute of Technology, Cambridge, MA 02139, USA*
[*]*xiaojun.wu@desy.de*

Abstract: Optical rectification with tilted pulse fronts in lithium niobate crystals is one of the most promising methods to generate terahertz (THz) radiation. In order to achieve higher optical-to-THz energy efficiency, it is necessary to cryogenically cool the crystal not only to decrease the linear phonon absorption for the generated THz wave but also to lengthen the effective interaction length between infrared pump pulses and THz waves. However, the refractive index of lithium niobate crystal at lower temperature is not the same as that at room temperature, resulting in the necessity to re-optimize or even re-build the tilted pulse front setup. Here, we performed a temperature dependent measurement of refractive index and absorption coefficient on a 6.0 mol% MgO-doped congruent lithium niobate wafer by using a THz time-domain spectrometer (THz-TDS). When the crystal temperature was decreased from 300 K to 50 K, the refractive index of the crystal in the extraordinary polarization decreased from 5.05 to 4.88 at 0.4 THz, resulting in ~1° change for the tilt angle inside the lithium niobate crystal. The angle of incidence on the grating for the tilted pulse front setup at 1030 nm with demagnification factor of −0.5 needs to be changed by 3°. The absorption coefficient decreased by 60% at 0.4 THz. These results are crucial for designing an optimum tilted pulse front setup based on lithium niobate crystals.

OCIS codes: (300.6495) Spectroscopy, terahertz; (320.7110) Ultrafast nonlinear optics; (260.3090) Infrared, far.

References and links

1. E. Balogh, K. Kovacs, P. Dombi, J. A. Fülöp, G. Farkas, J. Hebling, V. Tosa, and K. Varju, "Single attosecond pulse from terahertz-assisted high-order harmonic generation," Phys. Rev. A **84**(2), 023806 (2011).
2. T. Kampfrath, A. Sell, G. Klatt, A. Pachkin, S. Mährlein, T. Dekorsy, M. Wolf, M. Fiebig, A. Leitenstorfer, and R. Huber, "Coherent terahertz control of antiferromagnetic spin waves," Nat. Photonics **5**(1), 31–34 (2011).
3. S. Fleischer, Y. Zhou, R. W. Field, and K. A. Nelson, "Molecular orientation and alignment by intense single-cycle THz pulses," Phys. Rev. Lett. **107**(16), 163603 (2011).
4. T. Kampfrath, K. Tanaka, and K. A. Nelson, "Resonant and nonresonant control over matter and light by intense terahertz transients," Nat. Photonics **7**(9), 680–690 (2013).
5. L. Pálfalvi, J. A. Fülöp, G. Toth, and J. Hebling, "Evanescent-wave proton postaccelerator driven by intense THz pulse," Phys. Rev. **17**(3), 031301 (2014).
6. L. J. Wong, A. Fallahi, and F. X. Kärtner, "Compact electron acceleration and bunch compression in THz waveguides," Opt. Express **21**(8), 9792–9806 (2013).
7. W. R. Huang, E. A. Nanni, K. Ravi, K.-H. Hong, A. Fallahi, L. J. Wong, P. D. Keathley, L. E. Zapata, and F. X. Kärtner, "Toward a terahertz-driven electron gun," Sci. Rep. **5**, 14899 (2015).
8. E. A. Nanni, W. R. Huang, K.-H. Hong, K. Ravi, A. Fallahi, G. Moriena, R. J. Dwayne Miller, and F. X. Kärtner, "Terahertz-driven linear electron acceleration," Nat. Commun. **6**, 8486 (2015).

#251969 Received 14 Oct 2015; revised 27 Oct 2015; accepted 27 Oct 2015; published 4 Nov 2015

9. J. Á. Hebling, K.-L. Yeh, M. C. Hoffmann, and K. A. Nelson, "High-Power THz Generation, THz Nonlinear optics and THz Nonlinear Spectroscopy," IEEE J. Sel. Top. Quantum Electron. **14**(2), 345–353 (2008).
10. J. A. Fülöp, L. Pálfalvi, M. C. Hoffmann, and J. Hebling, "Towards generation of mJ-level ultrashort THz pulses by optical rectification," Opt. Express **19**(16), 15090–15097 (2011).
11. X. Wu, S. Carbajo, K. Ravi, F. Ahr, G. Cirmi, Y. Zhou, O. D. Mücke, and F. X. Kärtner, "Terahertz generation in lithium niobate driven by Ti:Sapphire laser pulses and its limitations," Opt. Lett. **39**(18), 5403–5406 (2014).
12. J. A. Fülöp, Z. Ollmann, C. Lombosi, C. Skrobol, S. Klingebiel, L. Pálfalvi, F. Krausz, S. Karsch, and J. Hebling, "Efficient generation of THz pulses with 0.4 mJ energy," Opt. Express **22**(17), 20155–20163 (2014).
13. K. Ravi, W. R. Huang, S. Carbajo, X. Wu, and F. Kärtner, "Limitations to THz generation by optical rectification using tilted pulse fronts," Opt. Express **22**(17), 20239–20251 (2014).
14. C. Vicario, A. V. Ovchinnikov, S. I. Ashitkov, M. B. Agranat, V. E. Fortov, and C. P. Hauri, "Generation of 0.9-mJ THz pulses in DSTMS pumped by a Cr:Mg_2SiO_4 laser," Opt. Lett. **39**(23), 6632–6635 (2014).
15. W. R. Huang, S. W. Huang, E. Granados, K. Ravi, K. H. Hong, L. Zapata, and F. X. Kärtner, "Highly efficient terahertz pulse generation by optical rectification in stoichiometric and cryo-cooled congruent lithium niobate," J. Mod. Opt. **62**(18), 1486–1493 (2015).
16. A.-L. Calendron, H. Çankaya, and F. X. Kärtner, "High-energy kHz Yb:KYW dual-crystal regenerative amplifier," Opt. Express **22**(20), 24752–24762 (2014).
17. http://www.rainbowphotonics.com/prod_dstms.php
18. http://www.unitedcrystals.com/LiNbO3.html
19. J. Hebling, G. Almási, I. Kozma, and J. Kuhl, "Velocity matching by pulse front tilting for large area THz-pulse generation," Opt. Express **10**(21), 1161–1166 (2002).
20. http://refractiveindex.info/?shelf=main&book=LiNbO3&page=Zelmon-o
21. O. Gayer, Z. Sacks, E. Galun, and A. Arie, "Temperature and wavelength dependent refractive index equations for MgO-doped congruent and stoichiometric $LiNbO_3$," Appl. Phys. B **91**(2), 343–348 (2008).
22. D. H. Jundt, "Temperature-dependent Sellmeier equation for the index of refraction, n_e, in congruent lithium niobate," Opt. Lett. **22**(20), 1553–1555 (1997).
23. S. W. Huang, E. Granados, W. R. Huang, K. H. Hong, L. E. Zapata, and F. X. Kärtner, "High conversion efficiency, high energy terahertz pulses by optical rectification in cryogenically cooled lithium niobate," Opt. Lett. **38**(5), 796–798 (2013).
24. L. Pálfalvi, J. Hebling, J. Kuhl, Á. Péter, and K. Polgár, "Temperature dependence of the absorption and refraction of Mg-doped congruent and stoichiometric LiNbO3 in the THz range," Appl. Phys. Lett. **97**, 123505 (2005).
25. M. Unferdorben, Z. Szaller, I. Hajdara, J. Hebling, and L. Pálfalvi, "Measurement of Refractive Index and Absorption Coefficient of Congruent and Stoichiometric Lithium Niobate in the Terahertz Range," J. Infrared Milli. Terahz. Waves, (in press).
26. L. Duvillaret, F. Garet, and J. L. Coutaz, "A reliable method for extraction of material parameters in terahertz time-domain spectroscopy," IEEE J. Sel. Top. Quantum Electron. **2**(3), 739–746 (1996).
27. T. D. Dorney, R. G. Baraniuk, and D. M. Mittleman, "Material parameter estimation with terahertz time-domain spectroscopy," J. Opt. Soc. Am. A **18**(7), 1562–1571 (2001).
28. L. Duvillaret, F. Garet, and J.-L. Coutaz, "Highly precise determination of optical constants and sample thickness in terahertz time-domain spectroscopy," Appl. Opt. **38**(2), 409–415 (1999).
29. U. T. Schwarz and M. Maier, "Frequency dependence of phonon-polariton damping in lithium niobate," Phys. Rev. B Condens. Matter **53**(9), 5074–5077 (1996).
30. Q. Liang, S. Wang, X. Tao, and T. Dekorsy, "Temperature dependence of free carriers and optical phonons in $LiInSe_2$ in the terahertz frequency range," Phys. Rev. B **92**(14), 144303 (2015).

1. Introduction

Terahertz (THz) radiation with extremely high peak field is important for many applications such as high harmonic generation [1], spin control [2], molecule alignment [3], time-resolved nonlinear spectroscopy [4], electron acceleration [5–8] *etc*. Among various THz generation methods, optical rectification with intra-pulse difference frequency generation is still the most efficient technique [9–13]. Percent level optical-to-THz energy conversion efficiencies have been demonstrated in organic crystals [14] and MgO-doped lithium niobate crystals [15]. For the next generation of strong field THz sources with mJ-level output energies, extremely high energy pump lasers with big spot size will be used [16]. However, organic crystals cannot be grown with big size and their low damage threshold limits the use of high power pump lasers [17]. Congruent lithium niobate crystals can be grown with extremely large crystal size with 2-inch in height (Z-axis) and also 2-inch in X-Y plane [18]. Furthermore, with MgO doping in the congruent lithium niobate, the damage threshold can be increased to 100 GW/cm^2. 2-inch congruent lithium niobate crystals with 6.0 mol% MgO doping level have been employed to generate THz radiation at 800 nm [11].

Using lithium niobate crystals for highly efficient generation of THz pulses, the tilted pulse front method is employed in order to achieve phase matching between the group

#251969 Received 14 Oct 2015; revised 27 Oct 2015; accepted 27 Oct 2015; published 4 Nov 2015

velocity of the infrared pump laser pulses and the phase velocity of the THz pulses [19]. The pump pulse intensity fronts are tilted after the pulses are illuminated on a grating and diffracted to the minus first order due to angular dispersion. In order to satisfy the phase matching condition, the crystal has to be cut with an angle calculated by the following formulas [19]

$$\begin{aligned} v_{opt}^{gr} \cdot \cos\theta &= v_{THz}^{ph} \\ n_{THz}^{ph} \cdot \cos\theta &= n_{opt}^{gr} \end{aligned} \tag{1}$$

Where θ is the apex angle of the crystal; v_{opt}^{gr} and v_{THz}^{ph} are the group velocity of the infrared pulses and phase velocity of the THz waves, respectively; n_{opt}^{gr} and n_{THz}^{ph} are the refractive indices for group velocity of infrared light and for phase velocity of THz waves, respectively. The refractive index for group velocity of infrared light is calculated by

$$n_{opt}^{gr} = n_{opt}^{ph} - \lambda_{opt} \cdot \frac{dn_{opt}^{ph}}{d\lambda_{opt}} \tag{2}$$

where n_{opt}^{ph} is the refractive index for phase velocity of the pump light and λ_{opt} is the optical pump wavelength [20]. The optical properties and parameters for congruent lithium niobate crystals can be found in references [21,22]. The refractive index of the phase velocity for lithium niobate crystals in the THz range is missing and needs to be carefully measured because it is crucial for calculating the apex angle of the crystal to achieve phase matching. Furthermore, when employing lithium niobate crystals for generating strong-field THz pulses, it is advantageous to cryogenically cool the crystal to reduce the linear absorption in the THz range [23]. However, the temperature will influence the refractive index of the crystal in the THz frequency range [24]. As a consequence, the apex angle of the crystal or the tilted pulse fronts needs to be modified to satisfy the phase matching condition [19]. Moreover, the absorption coefficient not only influences the out-coupling of the THz radiation but also has impact on the effective interaction length between the pump laser pulses and the generated THz pulses [10]. Knowing information of refractive index and absorption coefficient at different crystal temperatures is important to achieve high optical-to-THz efficiency.

In 2005, Pálfalvi *et al* reported temperature dependence of refractive index and absorption coefficient of different MgO doping levels in both stoichiometric and congruent lithium niobate crystals [24]. However, the refractive index and absorption coefficient values have some uncertainty due to the lensing effect caused by the curved surfaces of the crystals, and they were measured in only one polarization direction (the extraordinary polarization defined as the THz parallel to the Z-axis of the crystal). Furthermore, the measurement was carried out by a temperature-variable far-infrared Fourier transform spectrometer, and the lowest THz frequency in the experiment is 30 cm^{-1} (0.9 THz). The results of refractive index and absorption coefficient lower than 0.9 THz at different temperatures were unrevealed, which are essential in the intense THz generation by the tilted pulse front method. Although Unferdorben *et al* recently reported the measurements by using a THz time-domain spectrometer (THz-TDS) on a series of lithium niobate crystals with parallel surfaces [25], the results of temperature dependence are still lacking.

Here, we perform the first temperature dependent THz-TDS measurement on lithium niobate crystals over the frequency range of interest 0.3-1.9 THz. The temperature was varied from 300 K to 50 K in the THz-TDS system. We measured the refractive index and absorption coefficient for both ordinary (THz polarization parallel to the X-axis of lithium niobate crystal) and extraordinary polarizations (THz polarization parallel to the Z-axis) [25] at different crystal temperatures. Based on the temperature dependent measurements, we find that cryogenic cooling not only decreases the absorption for THz waves but also decreases the refractive index of the crystal in the THz frequency range, which makes the optimization

#251969 Received 14 Oct 2015; revised 27 Oct 2015; accepted 27 Oct 2015; published 4 Nov 2015

conditions for low temperature and room temperature not the same. To obtain higher optical-to-THz conversion efficiency at cryogenic cooling temperature, the apex angle of the crystals needs to be cut more accurately and the tilted pulse front setup needs to be built with a different incident angle on the grating for a specific pump laser wavelength.

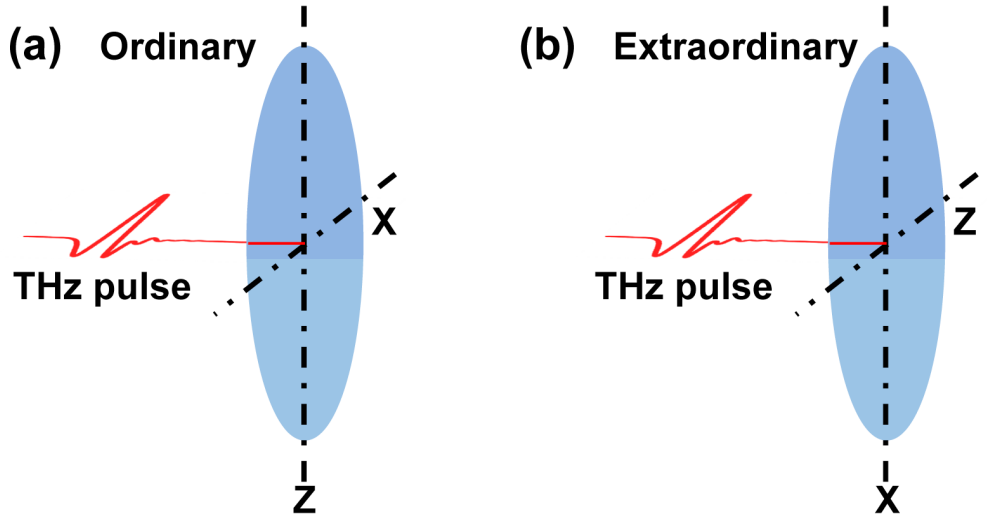

Fig. 1. Schematic of the transmission measurements of THz waves at different polarizations. (a) At ordinary polarization; and (b) At extraordinary polarization.

2. Experimental setup and sample description

We employed a home-made temperature-variable THz-TDS to measure our samples of congruent lithium niobate crystals. This system is pumped by a commercial Ti:Sapphire laser oscillator (Spectra-Physics) with 80 MHz repetition rate and 70 fs pulse duration. The THz emitter is a low-temperature grown GaAs antenna integrated with a Si hemisphere. The output THz pulses are focused onto the sample by two 90° off-axis parabolic mirrors and the transmission sample signal is refocused by another two parabolic mirrors onto the <110> ZnTe detector for electro-optic sampling. The THz propagation path including the GaAs generator and the ZnTe detector are in a vacuum chamber, which is pumped to a vacuum level of 10^{-5} mbar. The sample holder is specially designed for not only mounting the crystal but also cryogenic cooling the sample. The sample is connected to a thermostat and the cooling system is filled by liquid helium, but here the temperature can only be lowered down to 50 K due to some problems with the thermostat. When the chamber was pumped down and the temperature on the crystal has reached 50 K, we measured the emitted THz pulses through the four parabolic mirrors as a reference signal. The dynamic range of the THz-TDS, defined as the maximum THz signal divided by maximum noise value, is ~5000. We moved the sample into the THz focal plane and measured the transmitted signal after the crystal.

The congruent lithium niobate wafer is 6.0 mol% MgO-doped with 1.5 mm thickness in the Y-axis. The crystal is Y-cut with a marker cut parallel to the Z-axis. The X-Z plane is 1-inch in diameter which guarantees the sample can cover the focused THz beam (2-3 mm in diameter). In our measurement, we first measured the ordinary polarization defined as the THz polarization parallel to the X-axis and then rotated the crystal by 90° to measure the extraordinary polarization defined as the THz polarization parallel to the Z-axis of the wafer, as shown in Fig. 1.

3. Experimental results and discussion

For the THz-TDS measurement, we first measured a reference temporal waveform and then got a sample signal. These temporal waveforms give us the information for both amplitude

#251969 Received 14 Oct 2015; revised 27 Oct 2015; accepted 27 Oct 2015; published 4 Nov 2015

and phase. Without doing Kramers-Kronig transformation, we can easily calculate the refractive index and absorption coefficient based on the following formulas [26-28]:

$$
\begin{aligned}
n_2(\omega) &= \frac{\phi(\omega)c}{\omega d} + 1 \\
\kappa_2(\omega) &= \frac{-\ln\left(\rho(\omega)\cdot\frac{\left[n_2(\omega)+1\right]^2}{4n_2(\omega)}\right)c}{\omega d} \\
\alpha(\omega) &= 2\omega\kappa_2(\omega)/c
\end{aligned}
\tag{3}
$$

Where $n_2(\omega)$ is the frequency dependent refractive index; $\phi(\omega)$ is the phase difference; c is the speed of light in vacuum; ω is the angular frequency; d is the thickness of the sample; $\kappa_2(\omega)$ is the frequency dependent extinction coefficient; $\rho(\omega)$ is the amplitude ratio; $\alpha(\omega)$ is the absorption coefficient.

Fig. 2 (a) shows the temporal waveforms for vacuum reference and sample signals in extraordinary and ordinary polarizations measured at 50 K. The extraordinary signal is delayed by ~20 ps and the ordinary signal is delayed by ~28 ps compared to the reference signal. The phase difference indicates the refractive index of the sample since the thickness is fixed. The peak to peak value of the sample signal in the extraordinary polarization is reduced to only 35% of the reference signal, which means that the total loss was 65%. The refractive index for the extraordinary polarization is estimated to be 5.0, and then the Fresnel reflection loss can be estimated as 44% between the vacuum and the crystal surface. Therefore, there still exists ~21% absorption by the sample even the crystal has been cooled to 50 K. Similarly, if we implement the rough estimation for the ordinary polarization, its transmission is 19% and its total loss is 81%. The Fresnel reflection loss is ~54% (the refractive index here is estimated to be 6.5), resulting in ~27% absorption loss for ordinary polarization. The residual absorption loss can be further reduced by cooling the crystal to even lower temperature <50 K.

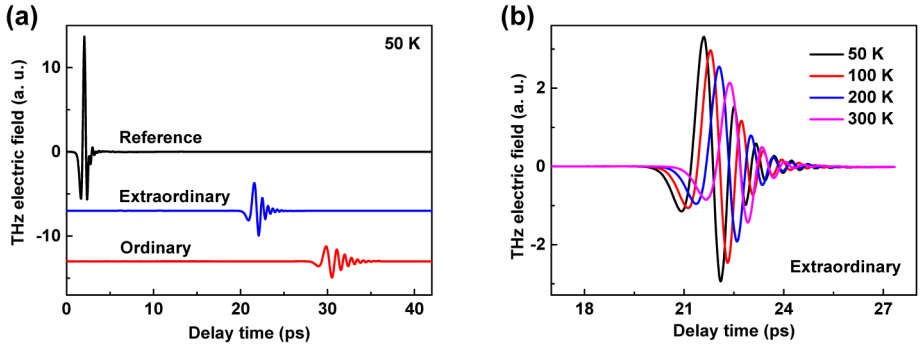

Fig. 2. (a) THz temporal waveforms for vacuum reference, extraordinary and ordinary polarization measured at a temperature of 50 K. (b) Temperature dependence of THz temporal waveforms for an extraordinary light.

#251969 Received 14 Oct 2015; revised 27 Oct 2015; accepted 27 Oct 2015; published 4 Nov 2015

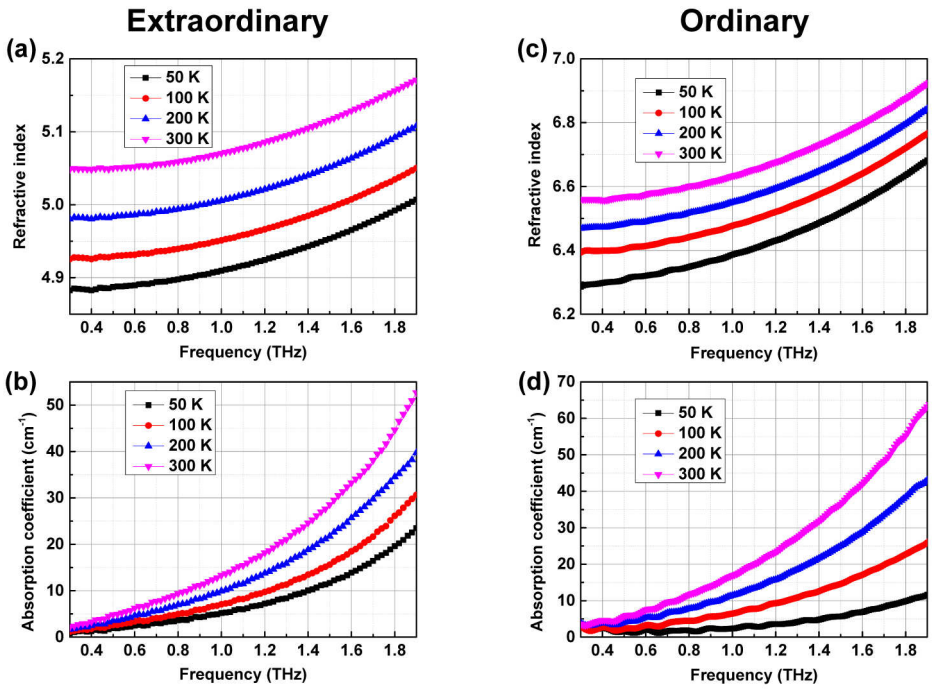

Fig. 3. Temperature dependence of refractive index and absorption coefficient for extraordinary polarization (a) and (b); ordinary polarization (c) and (d).

For more details of the variation of refractive index and absorption coefficient, we calculated them by using Eq. (3) and we plotted these curves shown in Fig. 3. For both extraordinary and ordinary polarizations at different temperatures, in Fig. 3 (a) and 3 (c), the refractive indices are higher for the higher THz frequencies in the frequency range 0.3-1.9 THz. Over the whole frequency range, the refractive index for both polarizations decreases with decreasing temperature.

For the absorption coefficient in Fig. 3 (b) and 3 (d), the THz absorption is higher for higher frequencies at all temperatures. Lithium niobate crystals have a phonon vibration at 7.7 THz which contributes the major absorption for our interest frequency range [29]. THz polarized along the ordinary shows a higher absorption coefficient than those polarized along the extraordinary polarization at 300 K. In order to clarify the variation of the refractive index and absorption coefficient with the temperature [30], we plot the differences in refractive index and absorption coefficient for extraordinary polarization as a function of the temperature change, shown in Fig. 4. For the three temperature variations, the refractive index difference keeps constant in 0.3-1.9 THz. However, the values are not the same. When the temperature decreases from 300 K to 200 K, the refractive index difference is ~0.06. It decreases by 0.05 when the temperature further decreases from 200 K to 100 K. For the last 50 K temperature change, it only decreases by 0.04. We summarize the temperature dependent refractive index and absorption coefficient at 0.4 THz and 1.6 THz in Table 1. For the extraordinary polarization, when the temperature decreases from 300 K to 50 K, the refractive index also decreases by ~0.16. The value increases to 0.26 for the ordinary polarization at 0.4 THz. The refractive index of the lithium niobate crystal can be fitted by a polynomial equation [24]:

$$n(\nu) = A + B\nu^2 + C\nu^4 \tag{4}$$

#251969 Received 14 Oct 2015; revised 27 Oct 2015; accepted 27 Oct 2015; published 4 Nov 2015

where ν is the frequency in the unit of THz, *n* is the refractive index, A, B, and C are the coefficients at different temperatures fitted from the measured data in Fig. 3, which were shown in Table 2. The fittings of 50 K are shown in Fig. 5.

Table 1. Temperature dependent refractive index and absorption coefficient for extraordinary and ordinary at 0.4 and 1.6 THz.

	Extraordinary				Ordinary			
	Refractive index		Absorption coefficient (cm^{-1})		Refractive index		Absorption coefficient (cm^{-1})	
Temperature	0.4 THz	1.6 THz	0.4 THz	1.6 THz	0.4 THz	1.6 THz	0.4 THz	1.6 THz
50 K	4.9	5.0	1.3	13.9	6.3	6.5	2.4	6.9
100 K	4.9	5.0	1.8	18.5	6.4	6.6	2.7	17.1
200 K	5.0	5.1	2.5	25.7	6.5	6.7	3.9	28.8
300 K	5.1	5.1	3.3	33.2	6.6	6.8	4.6	42.0

Table 2. A, B, and C coefficients for the refractive index polynomial equation of lithium niobate in extraordinary and ordinary at different temperatures.

Polarization	Temperature (K)	A	B (10^{-2} THz^{-2})	C (10^{-3} THz^{-4})
Extraordinary	50	4.9	3.0	1.7
Extraordinary	100	4.9	2.8	2.1
Extraordinary	200	5.0	2.8	2.4
Extraordinary	300	5.0	2.5	3.0
Ordinary	50	6.3	9.1	5.1
Ordinary	100	6.4	8.8	5.0
Ordinary	200	6.5	8.4	6.2
Ordinary	300	6.5	8.2	6.0

Figure 6 shows the temperature dependence of birefringence of lithium niobate crystal in the THz range. The data is obtained by using the refractive index of ordinary polarization to subtract those of extraordinary polarization. Birefringence of lithium niobate crystal can be used to design some THz devices and the temperature effect is helpful to improve the performance of lithium niobate based THz devices.

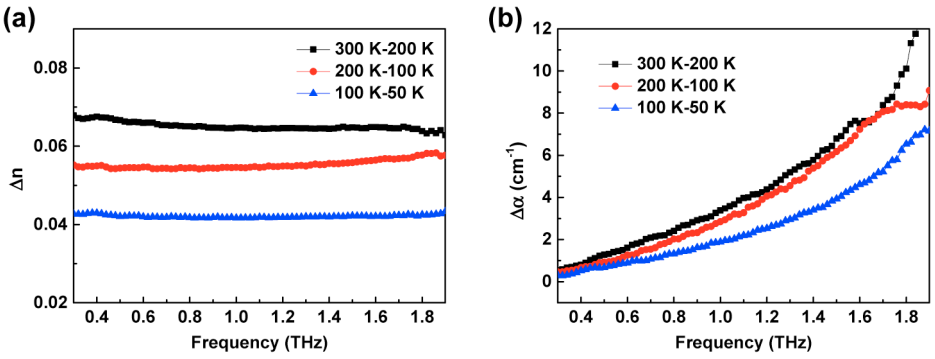

Fig. 4. Temperature dependence of (a) refractive index differences and (b) absorption coefficient differences for extraordinary polarization.

#251969 Received 14 Oct 2015; revised 27 Oct 2015; accepted 27 Oct 2015; published 4 Nov 2015

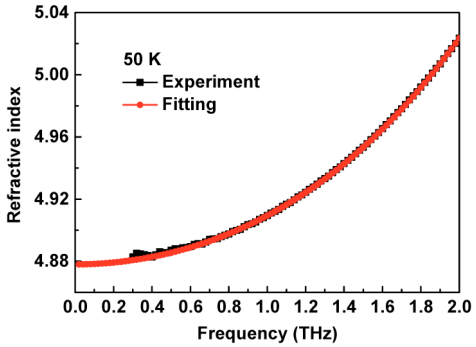

Fig. 5. Polynomial fit for extraordinary of the refractive index from 0.3 to 2 THz at 50 K.

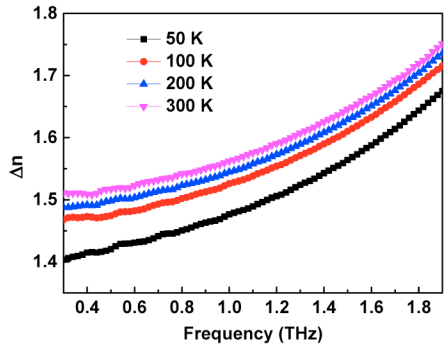

Fig. 6. Temperature dependence of birefringences in congruent lithium niobate crystal in the THz frequency range.

In order to clarify the influence of temperature to the tilted pulse front setup, we calculated the tilt angle inside the crystal to satisfy the phase matching condition. Here we assume the pump laser with 1030 nm wavelength and a grating with density 1500 lines/mm with a demagnification factor of −0.5. The group velocity index of infrared light is calculated by Eq. (2) where n_{opt}^{ph} is 2.2343 and $dn/d\lambda$ is −0.06567 μm^{-1} [20]. Figure 7 (a) exhibits the calculated phase matching angle from Eq. (1) as a function of temperature. At 50 K, the phase matching angle is 61.87° and it increases to 62.87° when the temperature increases to 300 K. This 1° phase matching angle difference will lead to ~3° variation of the incident angle for the grating, shown in Fig. 7 (b). That means it is necessary to change the grating angle, re-optimize the imaging system between the grating and the crystal and the crystal position at the cryogenic cooling temperature to achieve higher conversion efficiency.

#251969 Received 14 Oct 2015; revised 27 Oct 2015; accepted 27 Oct 2015; published 4 Nov 2015

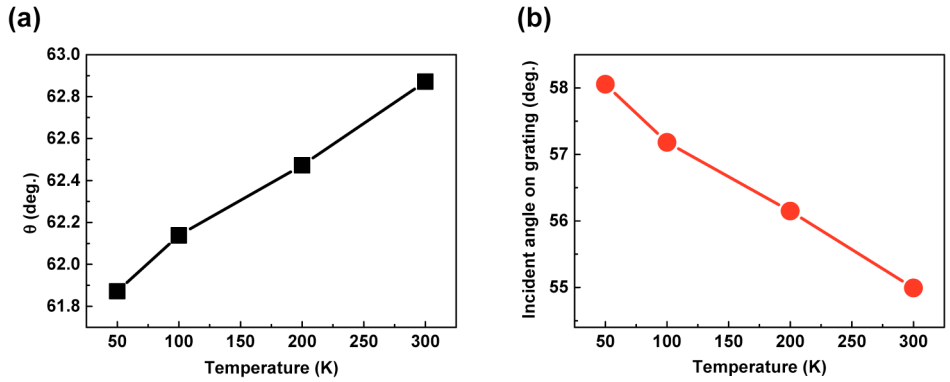

Fig. 7. Temperature dependence of (a) tilt angle in congruent lithium niobate crystal and (b) corresponding incident angle on grating. Pump wavelength: 1030 nm, grating density: 1500 lines/mm; demagnification factor: –0.5.

4. Conclusion

We performed a full temperature characterization of refractive index and absorption coefficient of 6.0 mol% MgO-doped congruent lithium niobate by using THz-TDS. We find that the refractive index decreases by 0.16 resulting in 1° variation for the phase matching angle of the crystal pumped by 1030 nm laser pulses. This change needs to be compensated by changing the incident angle on the grating by 3° or re-optimizing the imaging system. The absorption coefficient also decreases which makes the crystal to have a longer effective interaction length for lower temperature. Therefore, the crystal also needs to be re-optimized. These measurements are very helpful for strong-field THz generation and some other lithium niobate crystal based THz devices.

Acknowledgments

The authors acknowledge THz-TDS measurements under the help of Yanqi Liu, Dr. Tao Dong from Prof. Dr. Nan-lin Wang's group in Peking University. This work has been supported by the excellence cluster 'The Hamburg Centre for Ultrafast Imaging - Structure, Dynamics and Control of Matter at the Atomic Scale' of the Deutsche Forschungsgemeinschaft and the Center for Free-Electron Laser Science at the Deutsches Elektronen-Synchrotron (DESY), a Center of the Helmholtz Association. We acknowledge support from the European Research Council under the European Union's Seventh Framework Programme (FP/2007-2013) / ERC Grant Agreement n. 609920. W. Ronny Huang was supported by a National Defense Science and Engineering Graduate (NDSEG) Fellowship. Dr. Wu acknowledges support by a Research Fellowship from the Alexander von Humboldt Foundation.

#251969 Received 14 Oct 2015; revised 27 Oct 2015; accepted 27 Oct 2015; published 4 Nov 2015